DOI 10.5162/sensoren2019/6.4.5

Model based correction of motion deviations in the Planck-Balance

Huitian Bai [1], Norbert Rogge [2], Christian Rothleitner[3], Thomas Fröhlich[2]
[1] School of Precision Instruments and Opto-Electronics Engineering, Tianjin University, 92 Weijin Road, Nankai District, Tianjin, P.R.China
[2] Institute of Process Measurement and Sensor Technology, Technische Universität Ilmenau, 98684 Ilmenau, Germany
[3] Physikalisch-Technische Bundesanstalt, Bundesallee 100, 38116 Braunschweig, Germany

Tel.-Nr.: +86 13102030957, +493677691745, +495315921131
E-Mail: baihuitian@tju.edu.cn, norbert.rogge@tu-ilmenau.de, christian.rothleitner@ptb.de

Abstract

The Planck-Balance, a device planned to be used as a direct realization of the definition of the kilogram, utilizes the working principle of a Kibble balance [1]. Therefore, the motion of the coil under test has to be measured precisely. In the Planck-Balance, the coil is guided by the load carrier of a commercially available EMFC load cell. In order to reduce the measurement uncertainty of the velocity measurement, the tilt motions of this load carrier needs to be well known at the specified frequencies. The contribution presents different approaches to model the tilt of the load carrier during its sinusoidal excitation and the correction of tilt induced errors of the measurement.

Keywords: EMFC balance, mechanical simulation, tilt measurement, error correction, Kibble balance.

Introduction

In the Planck-Balance, a commercially available electromagnetic force compensated load cell (EMFC) is used to guide the moving coil of a voice coil actuator under test that is attached to the load carrier of the balance (see Figure 1). While the internal coil of the balance acts as a motor, which drives the system, the parallel lever system of the EMFC load cell provides a linear trajectory of the coil. This first mode of the experiment is utilized to determine the force factor Bl of the actuator under test (i.e. external voice coil), which is used to determine the mass of a weight in a second mode. The displacement of the coil and the induced voltage are measured as a function of time in order to calculate the force factor Bl as a ratio of the voltage and coil velocity. In the second mode the gravitational force produced by the weight is compensated by the force that is produced by the actuator when an electric current flows through the external coil.
Additional to the linear motion of the coil, the system also exhibits several tilt motions that cause errors in the velocity measurement if the displacement measurement system is not placed collinearly to the coil centre. These tilt motions should preferably be reduced as good as possible and the remaining tilt should be measured. In the experimental set up, three interferometer beams are used to measure the displacement of the load carrier and calculate two tilt angles from differences of the interferometer signals and the known distance between the laser spots. The induced voltage is measured with a digital voltmeter and the control algorithm is implemented on a commercially available digital signal processing system (DSP).

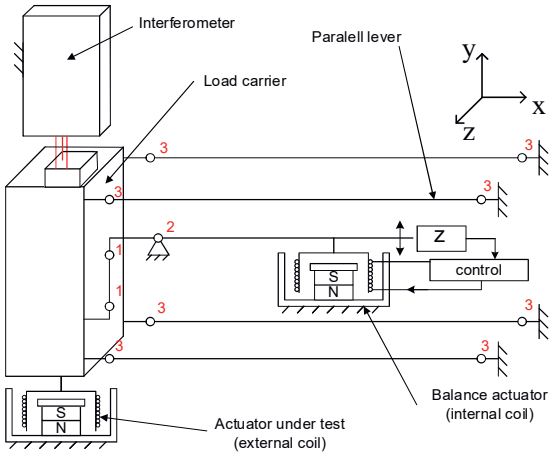

Figure 1: Schematic of balance and measurement set up.

Preceding investigations [2] indicated that the load carrier exhibits tilt oscillations when it is moved sinusoidal along the y-axis. The amplitude of these oscillations increases linear with the displacement amplitude and in a low frequency range of up to 50 Hz also with the excitation frequency.

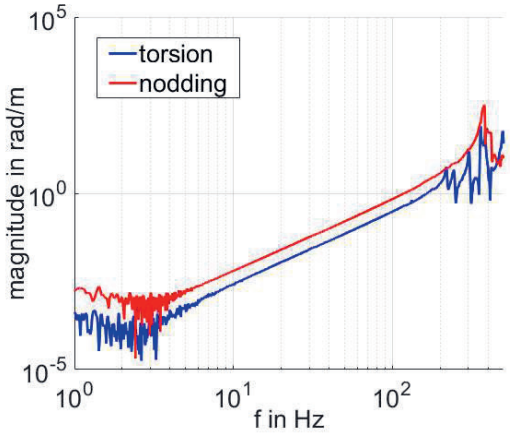

Figure 2: Torsion (blue) and nodding (red) tilt of the unloaded balance.

Furthermore, the mass distribution on the load carrier influences the amplitude of the oscillations themselves as well as the frequency range in which the increase is linear versus frequency. The frequency response of the system is obtained by exciting the system at the controller input with a chirp signal and applying the Fourier transform on the tilt signal and the displacement. Since the position sensor of this control system yields nonlinear characteristics, the applied chirp with frequencies of up to 30 Hz also produces higher harmonics, which can be used to identify also the system response for higher frequencies. The displacement acts as system input of the transfer system to make experiments with different excitation amplitudes comparable. An example of the occurring tilt amplitudes is shown in Figure 2, where “torsion” refers to the tilt about the x-axis, while the term “nodding” is used for rotations about the z-axis.

Model of the balance

In order to analyze the causes of the tilt oscillations, a model of the utilized balance is set up to investigate the sensitivity of the balances’ behavior versus the selected parameters. The model (shown in Figure 3) is mainly made up of four sections: mechanical system, position sensor, voice coil and U/I converter.

1. Mechanical subsystem:

The mechanical system is based on the CAD model and mechanical drawings of the device.

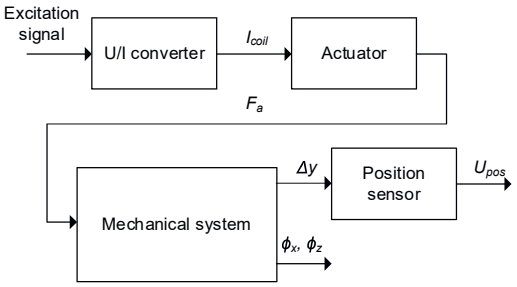

Figure 3: Main components of the balance model.

As proposed in [3] the mechanism is dissected into rigid bodies that are connected to each other by flexure hinges, which are simplified in Figure 1 as joints. The model contains two holders for putting on a mass piece, which are also available in the experimental set up of the tilt investigations and placed in a distance of 5 cm from the symmetry plane of the system. In the model, the position where the mass is located can be adjusted by setting the coordinates of the holders. The weight of the mass is defined by a constant and the unit of the constant is gram.

The joints in the model are assumed to possess different degrees of freedom, depending on their geometry and function within the system. The joints marked with number one in Figure 1 are able to rotate about the x-axis and z-axis, while the element between these two joints allows a deformation about the y-axis by adding another joint that is not shown in the schematic. The joints representing the lever bearing (number 2 in Figure 1) permit a rotation about the x-axis and z-axis, whereas the joints of the parallel lever system allow a rotational deformation about all axes and a translation along the x-axis.

The spring constants of the flexure hinges were calculated according to [4], where t, b and R represent geometrical parameters, α_z, Δy and Δx the deformation and M_z, F_y and F_x torque and applied forces, respectively, while E represents Young’s modulus:

Bending:
$$\frac{\alpha_z}{M_z} = \frac{9\pi R^{\frac{1}{2}}}{2Ebt^{\frac{5}{2}}} \quad (1)$$

Compression:
$$\frac{\Delta x}{F_x} = \frac{9\pi}{2Eb}\left(\frac{R}{t}\right)^{\frac{5}{2}} \quad (2)$$

Shear:
$$\frac{\Delta z}{F_z} = \frac{1}{Eb}\left[\pi\left(\frac{R}{t}\right)^{\frac{1}{2}} - 2.57\right]. \quad (3)$$

The additional rotational spring constants that cannot be calculated with the equations (1) to (3) were obtained by adjustment of their values

in order to fit to the measured behavior of the system.

2. Actuator subsystem:

The actuator subsystem of the model contains the electrical properties of the coil like its resistance and includes an interface between the mechanical and the electrical domain of the model. This interface is represented by the Bl of the internal coil of the balance that is the proportional factor of the relation between force F and the current I through the coil, as well as between the induced voltage U_{ind} and the coil velocity v:

$$Bl = \frac{U_{\mathrm{ind}}}{v} \tag{4}$$

$$Bl = \frac{F}{I} \tag{5}$$

The Bl of the internal coil was determined as 50 N/A in preceding experiments. Another parameter that plays an important role during the motion of the coil is the translational damping coefficient. It is determined as 9 N/(m/s) by fitting the model behavior to the experimental data. The mechanical part of the actuator system also contains the mechanical limits of the lever displacement, which is also present in the real system.

3. Position sensor:

The position sensor of the balance consists of a small aperture at the end of the transmission lever. The aperture partially blocks the light that is emitted by an infrared LED and that is pointed towards two photodiodes. Depending on the position of the aperture, the photodiodes produce photo currents that are equal, when both diodes receive the same amount of light. The difference of the photo currents is measured and converted into a voltage U_{pos}, which acts as the input signal for the lever position controller of the balance.
In order to control the displacement of the load carrier in the unit of meter instead of the position voltage, the relationship between them is considered. The load carrier displacement can be measured by the interferometer within the Planck-Balance set up. When the transmission lever is moving in a small angle, it is reasonable to assume from the geometry that the end of the transmission lever is displaced five times as much as the load carrier displacement and the directions of them are opposite. The function describing the relationship between the displacement of the end of the transmission lever relative to the balanced position and the position of load carrier is easily to get by fitting a polynomial to both signals.

4. U/I converter:

The U/I converter circuit board compares the voltage drop across a 500 Ω resistor to its voltage input, where the output current flows through the resistor and the actuator coil. The model of the converter also contains the saturation of the output current that depends on the limited voltage supply and the resistance of the load.

Model validation

To check the quality of the model, the measurements are carried out with a linear frequency chirp signal from 1 Hz to 30 Hz as input of the position controller and compared with simulations of the same input.

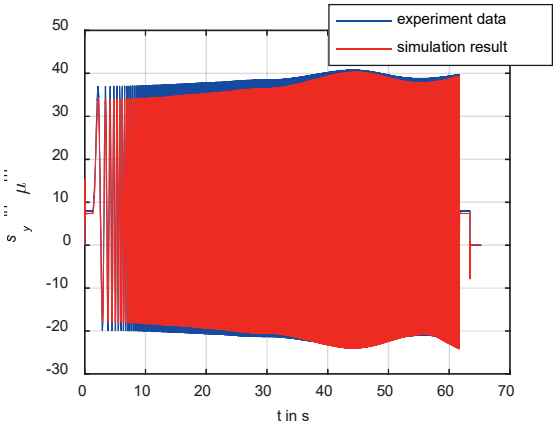

Figure 4: Displacement of the unloaded load carrier.

As depicted in Figure 4, the simulation of the displacement is in a quite good agreement with the measurement data, when the load carrier is unloaded. However, the torsion tilt oscillation does not appear in this case of simulation since the mechanical model is assumed perfectly symmetrical, which is in contrast to the real system.
The nodding oscillations do occur in the simulation with linear increase depending on the frequency (see Figure 5), but the amplitudes are smaller than the ones observed in the experiment.

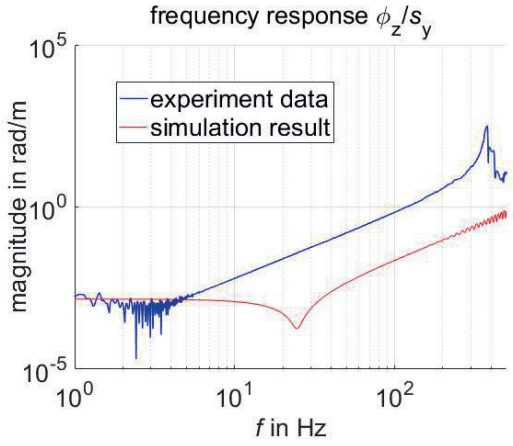

Figure 5: Nodding tilt amplitude relative to load carrier displacement, unloaded balance.

1. Mass distribution:

One parameter that is expected to be not symmetrical in the real system is the mass distribution on the load carrier. To quantify the influence of this parameter within the model, the model, as well as the balance, were loaded with a mass of 100 g in a distance of 5 cm relative to the symmetry plane. In this case, the simulation shows a linear increase of tilt amplitude not only for the nodding angle (Figure 6), but also for the torsion angle (Figure 7). In case of nodding, the simulated amplitudes are also significantly smaller. In addition to this, resonances occur around 50 Hz and 100 Hz, which are not present in the model due to the simplifications that were made to keep the focus on the linear tilt phenomena. For example, all levers in the model were assumed to be rigid bodies and do not possess elastic characteristics.

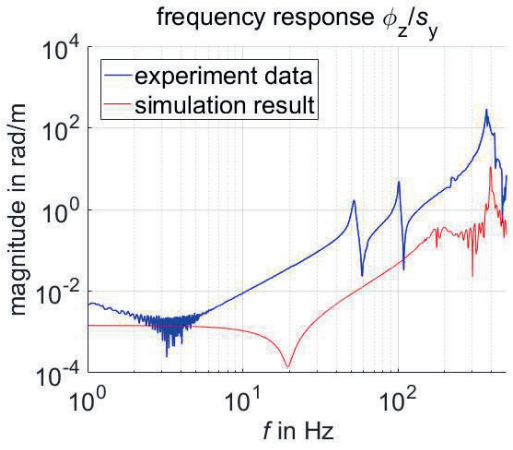

Figure 6: Nodding tilt amplitude relative to the load carrier displacement. The balance is loaded with 100 g on the right side.

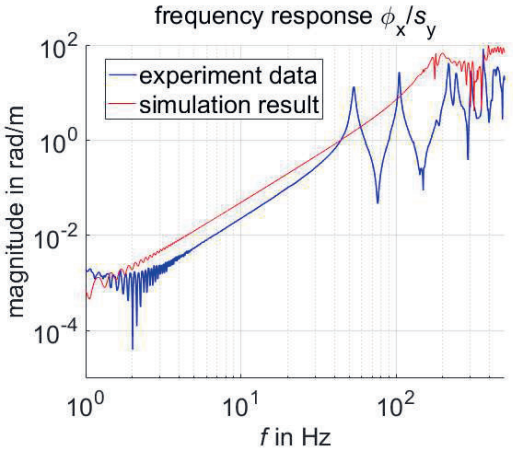

Figure 7: Torsion tilt amplitude relative to the load carrier displacement. The balance is loaded with 100 g on the right side.

In case of the torsion tilt, the frequency range with linear increase is more consistent with the measurement, but also only below the resonance effects.
In further simulations the mass of the unsymmetrically placed weight and its position in the xz-plane is varied to identify the linearity of the influence of these parameters on the behavior of the balance. Increasing the distance along the z-axis and the mass value, the amplitude linearly increases in the frequency range of 5 Hz to 30 Hz, while shifting the mass towards the actuator of the balance along x-axis decreases the amplitude. Furthermore, Figure 8 shows that the effect is not linear for a frequency of 30 Hz.

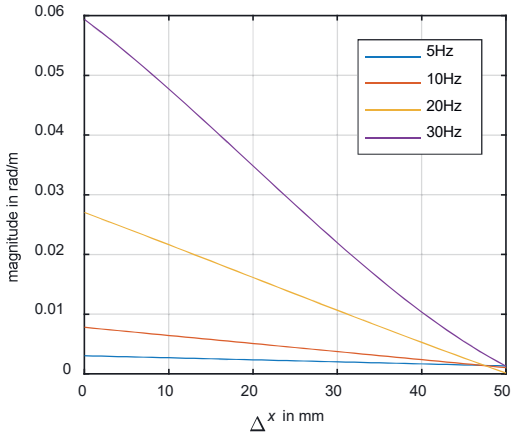

Figure 8: Relation between torsion tilt amplitude and weight placement along x-axis.

2. Joint stiffness:

The torsion tilt effects are not only caused by the unsymmetrical mass distribution, since they

also appear when the balance is unloaded and therefore the mass distribution can be assumed far more symmetrical than the state shown in Figure 7. Another possible cause for this type of tilt is the assumption, that not all joints possess the same spring constants. This influence is investigated by decreasing the rotational spring constants about the x- and z-axis and the translational spring constant along z-axis of one joint by a factor 10. As depicted in Figure 9, only the variation of the translational spring constant causes magnitudes close to the ones observed in the experiments.
The linearity of the influence of the translational spring constant along z-axis is checked in further simulations in which the value is varied in the range from 90 % to 99 % of the original value.

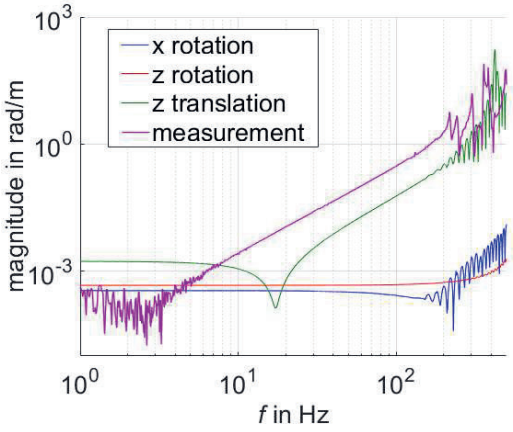

Figure 9: Torsion tilt amplitude response for decreased spring constant of one joint.

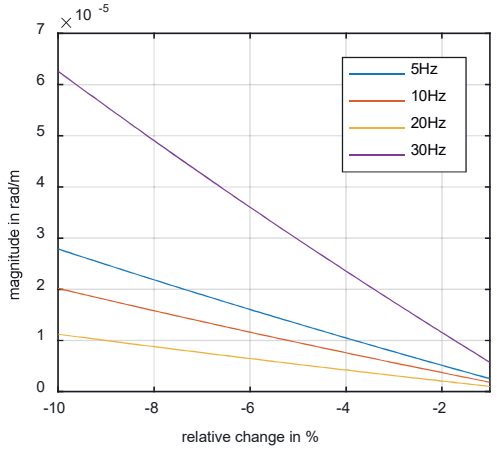

Figure 10: Torsion tilt amplitude for different translational spring constants of one joint.

The simulation results depicted in Figure 10 show a linear dependency for these small changes of the spring constant. The amplitude itself produced by this parameter a far too small to explain the results from the experiment and since the effect seems to be linear, it is not expected that other variations which are plausible according to the manufacturing tolerances can cause these effects.

Mounting deformation

An import factor that causes tilt oscillations is that the balance is mounted to the ground with three screws placed in the middle of the balance quiet close to each other. Since this fixation is expected to possess a finite stiffness, the mirror of the three beam interferometer was also placed onto the frame of the balance mechanism to examine the tilt of the mechanical reference frame to which the parallel lever system is connected to.
In this mode of the experiment, the measured tilt cannot be directly related to the load carrier displacement, since the interferometer only points to the frame of the balance. In case of a tilt that is caused by the chirp signal excitation with constant amplitude, a chirp signal is also expected for the tilt signal with an envelope corresponding to the transfer function of the tilt relative to the excitation amplitude. In order to obtain this transfer function, a chirp signal fit was applied to the tilt signals.

$$x(t) = A(t) \cdot \sin\left[2\pi \cdot \left(f_0 + \frac{k}{2} \cdot t\right) \cdot t + \varphi\right] \quad (6)$$

Equation (6) consists of the envelope function $A(t)$ multiplied with the chirp function, whose parameters are known since the signal is generated in the signal processing system. The envelope function is assumed as a second order polynomial and its parameters are estimated such that the chirp equation (6) fits to the measured chirp response within the tilt signal.
The transfer function of the tilt is then determined by dividing the envelope by the known excitation amplitude.
The results in Figure 11 show increasing tilt amplitudes for both types of tilt in the frequency range of up to 30 Hz. With the beforehand described method, it is not possible to obtain the frame tilt for higher frequencies, since it is not recommended to increase the frequency of the chirp due to the bandwidth of the utilized controller. In this range these amplitudes are smaller than the ones observed on the load carrier, but they represent a relevant portion of the load carrier tilt. This indicates that an improvement of the mounting design has the potential to reduce the tilt oscillations.

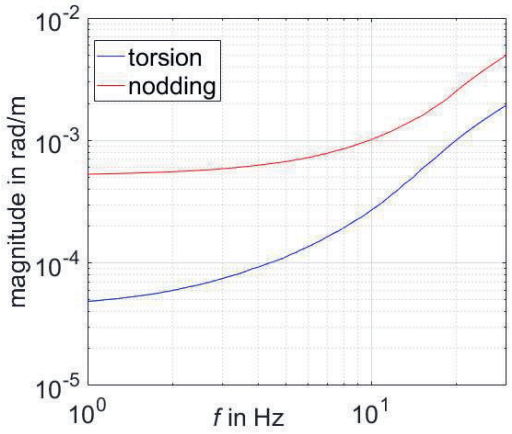

Figure 11: Amplitude transfer functions of the tilts measured on frame of the balance.

Bl determination

The preceding investigations can be utilized to improve further versions of the Planck-Balance set up. Nonetheless, also in the present set up the knowledge of the tilt motions is useful to correct the errors that are caused by them.
In the Planck-Balance set up, the motion that is performed to generate the induced voltage is sinusoidal in order to utilize the relatively small motion range of the load carrier of a commercially available EMFC balance. Assuming the sinusoidal nature of the displacement s and the induced voltage u, the Bl can be calculated from the displacement amplitude $\bar{S}$, the amplitude of the induced voltage $\bar{U}$ and the excitation frequency f_{sig}.

$$Bl = \frac{\bar{U}}{2\pi f_{\mathrm{sig}} \bar{S}} \tag{4}$$

The amplitudes are determined by fitting the parameters of a sinusoidal function with known frequency to the measured signals. The same fit can be used to obtain the amplitudes of the tilt signals that are derived from the signals of the three beam interferometer.
With the knowledge of the distances between the laser spots and the center of the actuator coil under test, the frequency dependency of the Bl determination can be reduced as depicted in Figure 12.

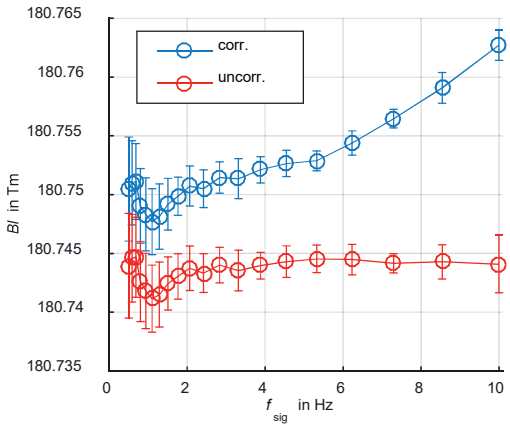

Figure 12: Relative change of the force factor Bl at different excitation frequencies.

Conclusion

This work presents investigations on two possible causes of the rotational motions that are observed in the velocity mode experiments of the Planck-Balance. This allows developing new approaches to decrease the amplitude of these motions. One option is to ensure a symmetrical mass distribution on the load carrier and shifting the center of gravity of the load carrier towards the middle of the balance. However, these measures should be done considering to keep the mass inertia small. Another reasonable method is to improve the mounting of the balance within its metrological frame. Nonetheless experiments show that a correction of the deviations caused by the tilt oscillations is feasible.

References

[1] C. Rothleitner, J. Schleichert, N. Rogge, L. Günther, S. Vasilyan, F. Hilbrunner, D. Knopf, T. Fröhlich and F. Härtig, "The Planck-Balance—using a fixed value of the Planck constant to calibrate E1/E2-weights," Measurement Science and Technology, vol. 29, no. 7, p. 074003, 2018.
[2] N. Rogge, J. Schleichert, C. Rothleitner, “Investigations on motion deviations of an EMFC balance”, Ilmenau Scientific Colloquium. Technische Universität Ilmenau; 59 (Ilmenau): 2017.09.11-15
[3] H. Weis, F. Hilbrunner, T. Fröhlich and G. Jäger, Parametric mechatronic model of a load cell with electromagnetic force compensation, IMEKO TC3 & TC5 & TC22 Int. Conf., pp 29–32, 2010.
[4] J. Paros, L. Weisbord. How to design flexure hinge. Mach Des 1965; 37:151–6.